Cellular Physiology and Biochemistry

Cell Physiol Biochem 2018;51:2324-2340
DOI: 10.1159/000495876
Published online: 7 December 2018
Accepted: 29 November 2018

Original Paper

Circular RNA circPVT1 Promotes Proliferation and Invasion Through Sponging miR-125b and Activating E2F2 Signaling in Non-Small Cell Lung Cancer

Xiuyuan Li[a] Zenglei Zhang[a] Hua Jiang[b] Qiang Li[b] Ruliang Wang[b] Hongliang Pan[b] Yingying Niu[c] Fenghai Liu[d] Hongmei Gu[c] Xingjun Fan[c] Jinxia Gao[e]

[a]Department of Respiratory, Hong Qi Hospital of Mudanjiang Medical College, Mudanjiang City, [b]Department of Radiology, Hong Qi Hospital of Mudanjiang Medical College, Mudanjiang City, [c]Department of Environmental Hygiene, School of Public Health, Mudanjiang Medical College, Mudanjiang City, [d]Department of Inspection and Quarantine, School of Public Health, Mudanjiang Medical College, Mudanjiang City, [e]Department of Prevention Medicine, School of Public Health, Mudanjiang Medical College, Mudanjiang City, China

Key Words
Non-small cell lung cancer • CircPVT1 • miR-125b • E2F2 • Proliferation • Invasion

Abstract
Background/Aims: Circular RNAs (circRNAs) are key regulators in the development and progression of human cancers, however its role in non-small cell lung cancer (NSCLC) tumorigenesis is not well understood. The aim of this study is to identify the expression level of circPVT1 in NSCLC and further investigated its functional relevance with NSCLC progression both *in vitro* and *in vivo*. ***Methods:*** Quantative real-time PCR was used for the measurement of circPVT1 in NSCLC specimens and cell lines. Fluorescence in situ hybridization analysis (FISH) assay was used for the identification of sublocation of circPVT1 in NSCLC cells. Bioinformatics analysis, luciferase reporter assay and RNA immunoprecipitation (RIP) were performed to verify the binding of c-Fos at circPVT1 promoter region, and the direct interaction between circPVT1 and miR-125b. Gain- or loss-function assays were performed to evaluate the effects of circPVT1 on cell proliferation and invasion. Western blot and immunohistochemistry assays were performed to detect the protein levels involved in E2F2 pathway. ***Results:*** We found that circPVT1 was upregulated in NSCLC specimens and cells. The transcription factor c-Fos binded to the promoter region of circPVT1, resulting in the overexpression of circPVT1 in NSCLC. Knockdown of circPVT1 suppressed NSCLC cell proliferation, migration and invasion, and increased apoptosis. In addition, circPVT1 mediated NSCLC progression via the regulation of E2F2 signaling pathway. More importantly, circPVT1 was predominantly abundant in the

Jinxia Gao

Department of Prevention Medicine, School of Public Health
Mudanjiang Medical College, Mudanjiang City, Heilongjiang Province (China)
E-Mail gaojinxiahlj@163.com

cytoplasm of NSCLC cells, and circPVT1 could serve as a competing endogenous RNA to regulate E2F2 expression and tumorigenesis in a miR-125b-dependent manner, which is further verified by using an *in vivo* xenograft model. ***Conclusion:*** circPVT1 promotes NSCLC cell growth and invasion, and may serve as a promising therapeutic target for NSCLC patients. Therefore, silence of circPVT1 could be a future direction to develop a novel treatment strategy.

Introduction

Lung cancer is one of the most malignant cancer types all over the world [1], with a low 5-year survival rate of 16.6% [2]. Non-small cell lung cancer (NSCLC) is the predominant form of lung cancer and accounts for the majority of cancer-related deaths in the world [3]. Conventional therapeutic strategies of chemotherapy following surgery showed limited effect for advanced NSCLC patients [4]. A better understanding of the molecular mechanisms underlying NSCLC progression and developing personalized therapeutic strategies are urgently needed to improve NSCLC prognosis.

With the advent of high-throughput sequencing and bioinformatic analysis, thousands of circular RNAs (circRNAs) have been successfully identified in multiple cell lines and across various species [5, 6]. CircRNAs are a large class of endogenous RNAs that are formed by exon skipping or back-splicing events with neither 5' to 3' polarity nor a polyadenylated tail; however, they attracted little attention until their function in post-transcriptional regulation of gene expression was discovered. CircRNAs are conserved and stable, and numerous circRNAs seem to be specifically expressed in a cell type or developmental stage [7, 8]. The progressive stage- and subcellular type- based expression modern indicate that circRNAs may play important roles in the mediation of multiple diseases, including cancer [9, 10]. Recently, certain kinds of circRNAs have been found to be significantly deregulated in NSCLC, and these deregulated circRNAs are suggested to participate in cancer development [11]. To date, elucidating the deregulated circRNAs and identifying their functions in NSCLC are still an ongoing process in cancer investigation.

Recent studies have shown that PVT1 gene, which is located on chromosome 8q24, a cancer susceptibility locus, plays an important role in human cancer via the regulation of protein stability of important oncogenes [12, 13]. The PVT1 gene is frequently up-regulated in many types of cancers, including NSCLC [14]. CircPVT1 is a circular RNA derived from one exon of the PVT1 gene and flanks two long introns (35269 bp and 41466 bp), which harbor many Alu repeats and may facilitate circPVT1 formation. CircPVT1 was first identified as circ6 by Memczak et al. [15] and then named circPVT1 after its host gene PVT1 in subsequent work [16-18]. They demonstrated that circPVT1 plays an oncogenic role in gastric cancer and head and neck squamous cell carcinoma, however, the specific role of this circular RNA is largely unknown, including NSCLC.

CircRNAs may function as competing endogenous RNAs (ceRNAs), thus inducing the release of genes that are targeted by specific miRNAs [19]. In this study, we hypothesized that circPVT1 regulated NSCLC proliferation, invasion and metastasis through sponging miR-125b and activating E2F2 signaling pathway. To verify this hypothesis, we detected the expression level of circPVT1 in NSCLC tissues and cell lines. By performing *in vitro* and *in vivo* experimental assays, we further investigated the functional relevance of circPVT1 with NSCLC progression.

Materials and Methods

Clinical samples

In total, forty-five serum samples, sixty-eight cancer tissues and paired adjacent noncancerous tissues from primary NSCLC patients were collected at Red Flag Hospital of Mudanjiang medical college between Jan 2013 and Jun 2017. Meanwhile, serum samples from forty-five healthy individuals were also collected. All the patients were pathologically confirmed and the tissues were collected immediately after they were obtained during the surgical operation, and then stored at -80°C to prevent RNA loss. In addition, 5 mL of venous blood from each participant was collected by vena puncture before chemotherapy was started. Serum was segregated via a centrifugation at 1600×g for 10 min at room temperature within 2 hours after collection, followed by a second centrifugation at 12000×g for 10 min at 4°C to remove the residual cells debris. Each serum supernatant was transferred into RNase free tubes and stored at -80°C until use. Written informed consent was obtained from each participant prior to blood collection. The study protocol was approved by the Clinical Research Ethics Committee of Hong Qi Hospital of Mudanjiang medical college.

Cell culture

The human NSCLC cell lines (A549, H292, SPC-A1, H1299, H1650, H1975, SK-MES-1) and one normal human bronchial epithelial cell line (HBE) were purchased from Chinese Academy of Sciences (Shanghai, China), cultured in DMEM (Gibco-BRL) medium supplemented with 10% fetal bovine serum (FBS), 100 U/ml penicillin and 100 mg/ml streptomycin (Invitrogen, Carlsbad, CA, USA) at 37°C in a humidified incubator with 5% CO_2.

RNA oligoribonucleotides and cell transfection

The small interfering RNA against circPVT1 (si-circPVT1), c-Fos (si-c-Fos) and negative control (si-NC), miR-125b mimics and NC mimics were synthesized by GenePharma (Shanghai, China). The coding sequence of c-Fos and E2F2 along with control sequences were amplified, cloned into pcDNA3.1 vector. The lentivirus vector containing circPVT1 overexpression plasmid (Lv-circPVT1) or negative control vector (Lv-NC) was amplified and cloned by GeneChem (Shanghai, China). pre-miR125b encompassing the stem-loop was amplified and then cloned into a lentiviral vector (Lv-miR-125b), and a lentiviral vector expressing a scramble RNA was used as the control (Lv-Sc). Cells were plated at 5×10^4 cells/well in 24-well plates approximately 24 h before transfection. After the cells reached 30-50% confluence, transfection was carried out using Lipofectamine 3000 (Invitrogen) following the manufacturer's instructions. Transfection efficiency was evaluated in every experiment by RT-qPCR 24 h later to ensure that cells were actually transfected. Functional experiments were then performed after sufficient transfection for 48 h. The sequences of small interfering RNAs are shown in Table 1.

Table 1. Information of the RT-qPCR primer sequences and siRNA sequences

RT-qPCR primer name	primer sequence (5'-3')
CircPVT1 (Forward)	CGACTCTTCCTGGTGAAGCATCTGAT
CircPVT1 (Reverse)	TACTTGAACGAAGCTCCATGCAGC
E2F2 (Forward)	GAACGAGTCCCTCTTCACTTTC
E2F2 (Reverse)	GTTCCGATCTGCTGCATATAACT
miR-125b (Forward)	ACCCAGTGCGATTTGTCA
miR-125b (Reverse)	ACTGTACTGGAAGATGGACC
c-Fos (Forward)	TGGCAGCAGTACCAATGGC
c-Fos (Reverse)	CCAGGCTGAGGAGTGGTACT
GAPDH (Forward)	GCACCGTCAAGGCTGAGAAC
GAPDH (Reverse)	ATGGTGGTGAAGACGCCAGT
U6 (Forward)	CTCGCTTCGGCAGCACA
U6 (Reverse)	AACGCTTCACGAATTTGCGT
U1 (Forward)	GGGAGATACCATGATCACGAAGGT
U1 (Reverse)	CCACAAATTATGCAGTCGAGTTTCCC
ChIP-qPCR primer name	primer sequence (5'-3')
P1 (Forward)	TTGGTGGTCTAGAACATTCT
P1 (Reverse)	GGTACTGTATACCCTTAATA
P2 (Forward)	AAATACATATTCATAGAAGT
P2 (Reverse)	TCGGTAGTTGTCTCTTACCA
siRNA name	siRNA sequence (5'-3')
si-circPVT1 #1	GCAAAUGAAAGCUACCAAUTT
si-circPVT1 #2	GCACAAUAUCUUUGAACUATT
si-circPVT1 #3	CUAGAAUCCUAAAGGCAAATT
si-c-Fos	CCGGAGGAGGGAGCUGACUTT
si-NC	UUCUCCGAACGUGUCACGUTT

RNA extraction and reverse transcription-quantitative PCR (RT-qPCR)

Extraction of RNA from tissue samples and cell fraction was performed using Trizol (Invitrogen) according to the manufacturer's protocol. Total serum RNA was extracted by using the commercial miRNeasy Serum/Plasma kit (Qiagen, Waltham, MA). All RNA elution steps were carried out at 12000×g for 15s, and the RNA was finally eluted in 15 μl RNase-free ultra-pure water. RNA was reverse transcribed using the SuperScript III® (Invitrogen) and then amplified by RT-qPCR based on the TaqMan method on an BioRad CFX96 Sequence Detection System (BioRad

company, Berkeley, CA). The gene expression levels were normalized by GAPDH (for mRNAs and circPVT1) or U6 expression (for miR-125b). RT-qPCR results were analyzed and expressed relative to CT (threshold cycle) values, and then converted to fold changes. All the premier sequences were synthesized by RiboBio Inc. (Guangzhou, China), and their sequences are shown in Table 1.

Immunofluorescence

Cell on slides were permeabilized with 0.3% Triton X-100 for 15 min after being fixed with 4% paraformaldehyde. Then goat serum was used for blocked, and then cells were incubated with anti-c-Fos antibody (#2250, 1:100, Cell Signaling Technology, Cambridge, MA) for overnight at 4°C The slides were then incubated with anti-rabbit Alexa Fluor 488 (Jackson Immunoresearch, West Grove, PA, USA) for 1 hr under room temperature. DAPI was used for nuclear counterstaining. The samples were observed under a fluorescence microscope (DMI4000B, Leica). Positive cells were counted blindly in a ×40 magnification.

Fluorescence in situ hybridization analysis (FISH)

Specific circPVT1 probe (5'-CATTCGTGAACGAATACAATCTGGAACA-3'-) was synthesized by Sangon Biotech (Sangon Biotech (Shanghai) Co., Ltd). Nuclear and cytosolic fraction separation was performed using a PARIS kit (Life Technologies), and RNA FISH probes were designed and synthesized by Bogu according to the manufacturer's instructions. Briefly, cells were fixed in 4% formaldehyde for 15 min and then washed with PBS. The fixed cells were treated with pepsin and dehydrated through ethanol. The air-dried cells were incubated further with 40 nM of the FISH probe in hybridization buffer. After hybridization, the slide was washed, dehydrated and mounted with Prolong Gold Antifade Reagent with DAPI for detection. The slides were visualized for immunofluorescence with a fluorescence microscopy (DMI4000B, Leica).

Signal transduction reporter array

Cignal 45-Pathway Reporter Array (Qiagen) was used to simultaneously investigate alternations in the activities of 45 canonical signaling pathways in response to knockdown of circPVT1. Cells were transfected with si-circPVT1 #1 for 24 h and were subsequently transfected with a mixture of a transcription factor-responsive firefly luciferase reporter and a constitutively expressing Renilla construct. The relative activity of each pathway was decided by luciferase/Renilla and normalized by untreated controls.

RNA immunoprecipitation (RIP) and Chromatin immunoprecipitation (ChIP)

Magna RIP™ RNA-Binding Protein Immunoprecipitation Kit (Millipore, Billerica, MA, USA) were used for RIP. NSCLC cells were lysed in complete RNA lysis buffer, then cell lysates were incubated with RIP immunoprecipitation buffer containing magnetic beads conjugated with human anti-Argonaute2 (AGO2) antibody (Abcam, ab32381), anti-E2F2 (Abcam, ab65222) or negative control mouse IgG (Millipore). EZ ChIP Chromatin Immunoprecipitation Kit (Millipore) and anti-c-Fos antibody (#2250, Cell Signaling Technology, Cambridge, MA) were used for ChIP according to the manufacturer's protocol.

Cell proliferation assay

The changed cell viability after transfection was assayed using the CCK8 Kit (Dojindo, Rockville, MD, USA). In brief, NACLC cell lines were seeded into a 96-well plate in triplicate and then treated with serial types of siRNAs for 48 h. After, cell cultures were treated with the CCK8 reagent and further cultured for 2 h. The optical density at 450 nm was measured with a spectrophotometer (Thermo Electron Corporation, MA, USA). The percentage of the control samples of each cell line was calculated thereafter.

Flow cytometry for apoptosis analysis

Cells were collected after transient transfection for 24 hr, then washed with PBS and trypsin containing 0.25% trypsin-EDTA to get the single-cell suspensions. They were then fixed in ice-cold 70% ethanol and with Annexin-V FITC and propidium iodide (PI) solution (Sigma-Aldrich; Merck KGaA, Darmstadt, Germany). Apoptosis was detected by on a BD FACSCalibur instrument.

TUNEL assay

TUNEL staining was performed to evaluate cell apoptosis. In brief, different group of cells were fixed by using 4% formaldehyde. Cells were fixed and stained with TUNEL kit according to the manufacturer's instructions (Vazyme, TUNEL Bright-Red Apoptosis Detection Kit, A113). TUNEL-positive cells were counted under fluorescence microscopy (DMI4000B, Leica).

Cell migration and invasion assays

Cell migration was evaluated by performing wound healing assay. Wounds were scratched on the monolayer of cells using 20 μl pipette tips. Plates were washed once with fresh medium to remove non-adherent cells after the cells had been cultured for 48 h, and then photographed. Cell invasion ability was tested by using transwell invasion assay. Briefly, 100 μl matrigel (BD, USA) was firstly added onto the bottom of the transwell chamber (24-well insert; 8-mm pore size, Corning Costar Corp), then 1×10^5 NSCLC cells in reduced serum medium (Opti-MEM, Gibco) were placed on the coated membrane in the chamber. Cells that migrated through the permeable membrane were fixed in methanol, stained with crystal violet, and counted under a microscope at 20× magnification in random fields in each well.

In vivo tumorigenesis assay

Male BALB/C nude mice (6 weeks of age) were purchased from Shanghai SIPPR-BK Laboratory Animal Co. Ltd. (Shanghai, China) and maintained in microisolator cages. 1×10^7 A549 cells transfected with Lv-circPVT1 and (or) Lv-miR-125b were suspended in 110 μl of serum-free DMEM, and then injected subcutaneously in the flank. Four weeks later, the xenograft tumor was stripped and the size was calculated.

Western blots and antibodies

Cell lysates were prepared with RIPA buffer containing protease inhibitors (Sigma). Protein concentrations were measured with the BCA Protein Assay according to the manufacturer's manual (Beyotime Institute of Biotechnology, Shanghai, China). Equal amounts of protein were separated by 10% sodium dodecyl sulfate-polyacrylamide gel electrophoresis and were transferred to polyvinylidene fluoride membranes (Millipore, Billerica, MA). Membranes were incubated overnight at 4 °C with a 1:1000 solution of antibodies (Cell Signaling Technology). A secondary antibody was then used for immunostaining for one hour at room temperature. The primary antibodies used here are anti-c-Fos antibody (Abcam, ab208942, 1:1000, Cambridge, MA), anti-E2F2 antibody (Abcam, ab65222, 1:1000), anti-E2F1 antibody (Abcam, ab179445, 1:1000), anti-E2F3 antibody (Abcam, ab50917, 1:1000), anti-pRb (S795) antibody (Abcam, ab47474, 1:1000), anti-cyclin-D1 antibody (Abcam, ab16663, 1:1000), anti-RYBP antibody (Abcam, ab5976, 1:1000) and anti-β-actin antibody (Abcam, ab8227, 1:1000).

Statistical analysis

Kolmogorov-Smirnov test was used to determine the normality of the distribution of data in each group. Count dates were described as frequency and examined using Fisher's exact test. The Mann-Whitney U test or Kruskal-Wallis test was used for evaluating the difference among clinical cohort groups or cell groups. All statistical analyses were performed with SPSS 17.0 software (SPSS Incorporation, Chicago, IL). Error bars in figures represent SD (Standard Deviation). The results were considered statistically significant at $P < 0.05$.

Results

CircPVT1 is upregulated in NSCLC and can serve as effective diagnostic indicator

To investigate whether the expression of circPVT1 is altered in NSCLC, we detected the expression of circPVT1 in 68 NSCLC tissues and paired adjacent non-tumor tissues. As shown in Fig. 1A, a significant elevated expression of circPVT1 was identified in NSCLC tissues when compared to matched non-tumor tissues. In addition, 60.3% (41 of 68) cases had at least 2-fold higher expression of circPVT1 in NSCLC tissues in contrast to paired normal tissues (Fig. 1B). Also, we examined the expression of circPVT1 in serum samples obtained from another independent cohort of 45 NSCLC patients and 45 healthy individuals. As

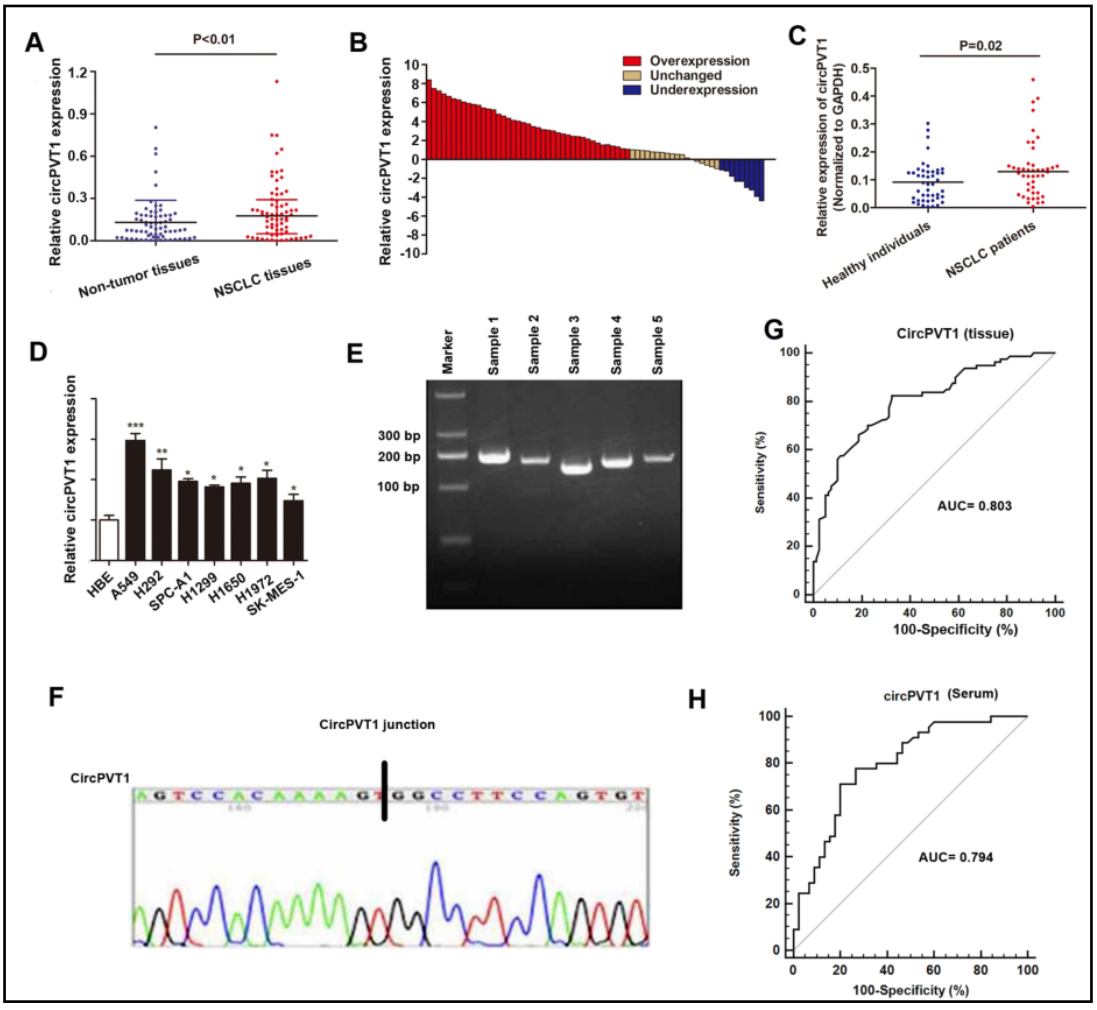

Fig. 1. Identification of circPVT1 as diagnostic factor in NSCLC. A Expression of circPVT1 in primary NSCLC tissues and non-tumor tissues was detected by RT-qPCR. B. The circPVT1 expression level was analyzed using RT-qPCR and expressed as $\log_2$ fold change (NSCLC/normal), and the $\log_2$ fold changes were presented as follows: >1, overexpression (41 cases); <1, underexpression (18 cases); the remainder were defined as unchanged (9 cases). C. Serum circPVT1 expression was tested via RT-qPCR. D. Expression level of circPVT1 in NSCLC cell lines and normal HBE cells were determined. E. The RT-qPCR product of circPVT1 was visualized by electrophoresis in ethidium bromide-stained 2.5% agarose gels. F. RT-qPCR products were purified and sequenced to confirm circPVT1 junction sequences. G-H. Diagnostic efficacy of circPVT1 in NSCLC tissue (G) or serum samples (H) was detected via ROC curve analysis. *P<0.05, **P<0.01, ***P<0.001.

expected, circPVT1 was also upregulated in serum of NSCLC patients than healthy controls (Fig. 1C). Furthermore, circPVT1 also showed an increased expression in seven NSCLC cell lines (A549, H292, SPC-A1, H1299, H1650, H1975, SK-MES-1) than in HBE cells, which is a human bronchial epithelial cell line (Fig. 1D). The circPVT1 PCR products from 5 NSCLC tissue samples were assessed on agarose gels to confirm that a specific circRNA species was amplified (Fig. 1E), and further verified by DNA sequencing to confirm the amplification of the specific circRNA junction (Fig. 1F).

We then evaluated the diagnostic value of circPVT1 expression in tissues and serum of NSCLC patients. The ROC analysis showed an area under curve (AUC) of 0.803, with a diagnostic sensitivity and specificity reaching 82.5% and 67.5% (95% CI = 0.733-0.861) for circPVT1 expression in tissues (Fig. 1G), and the AUC, diagnostic sensitivity and specificity were 0.794, 71.1% and 80.0% for serum circPVT1 expression, respectively (Fig. 1H). This

indicates that serum circPVT1 has a potential to serve as a biomarker for NSCLC diagnosis. Analysis of association between circPVT1 expression and clinical pathological factors of 68 primary tissue samples revealed that circPVT1 expression was positively correlated with distant metastasis, but not with other factors, such as gender, age, tumor size, TNM stage and histological grade (Table 2). This indicates a potential prognostic significance of circPVT1 for NSCLC patients.

Table 2. Clinical characteristics of 68 patients and the expression of circPVT1 in primary NSCLC tissues

Characteristics	Case	circPVT1 Median (Range)	P-Value
Age			0.569
<55	34	0.11 (0.02-0.67)	
≥55	34	0.16 (0.06-0.51)	
Gender			0.675
Male	43	0.12 (0.03-0.72)	
Female	25	0.17 (0.01-0.67)	
Tumor size			0.351
<3cm	39	0.17 (0.04-0.52)	
≥3cm	29	0.12 (0.01-0.73)	
Histological grade			0.106
Well	21	0.13 (0.01-0.64)	
Moderate	37	0.17 (0.05-0.61)	
Poor	10	0.19 (0.08-0.77)	
Distant metastasis			0.004
Positive	17	0.38 (0.10-0.82)	
Negative	51	0.12 (0.01-0.59)	
TNM stage			0.052
I- II	31	0.11 (0.01-0.75)	
III-IV	37	0.16 (0.06-0.82)	

CircPVT1 is actively induced by c-Fos in NSCLC cells

Increasing evidence has revealed that several key transcription factors contribute to RNA dysregulation in the human cancer cells, to this end, we searched for transcription factors that might be linked to circPVT1 deregulation. Using the online transcription factor prediction software JASPAR (http://jaspar.genereg.net/), we found that there are two c-Fos sites in the circPVT1 promoter regions with high score (Fig. 2A). Experimental validation using RT-qPCR showed that c-Fos expression was highly expressed in NSCLC cells when compared to HBE cells at both transcript and protein levels (Fig. 2B). The upregulation of c-Fos level was further confirmed in 3 random selected NSCLC tissues compared to the paired non-tumor tissues (Fig. 2C). Moreover, transfection of c-Fos overexpression vector (Fig. 2D) dramatically increased circPVT1 expression levels in A549 and H292 cells (Fig. 2E), while knockdown of c-Fos (Fig. 2F) showed an opposite effect (Fig. 2G). Consistently, immunofluorescence assay showed that c-Fos was much more enriched in the nucleus of A549 cells when compared to HBE cells (Fig. 2H). We also performed ChIP assay to further verify the enrichment of c-Fos at promoter region of circPVT1 with specific primers. As expected, c-Fos was enriched at promoter region of circPVT1 in NSCLC cells (Fig. 2I). In addition, the circPVT1 promoter region including 2 potential binding sites of c-Fos was inserted into a PGL3 luciferase reporter vector, and dual-luciferase reporter analysis showed that c-Fos promoted the luciferase activity at both sites of circPVT1 promoter region (Fig. 2J). These results indicated that the upregulation of circPVT1 in NSCLC may be induced by c-Fos.

Knockdown of circPVT1 suppresses cell proliferation and invasion in vitro

The functional role of circPVT1 in NSCLC progression was then investigated. We first blocked the expression of circPVT1 in A549 and H292 cells by transfecting with circPVT1 siRNA. The specific siRNA which covers back-splicing region of circPVT1 was constructed (Fig. 3A). As shown in Fig. 3B, si-circPVT1 #1 showed the highest silencing efficiency and was chosen for transfection assays. Subsequently, the effect of circPVT1 on NSCLC progression were examined. CCK8 assay showed that knockdown of circPVT1 significantly inhibited cell proliferation rate when compared to control vectors in both cell lines (Fig. 3C). Cell-cycle assays indicated that knockdown of circPVT1 caused cell-cycle arrest in G0/G1 phase (Fig. 3D). Meanwhile, an increased proportion of apoptotic nucleus was induced by knockdown of circPVT1 as shown by TUNEL assay (Fig. 3E). In addition, knockdown of circPVT1 also decreased the migratory ability of NSCLC cells as shown in wound-healing assay (Fig. 3F). Matrigel invasion assay showed that knockdown of circPVT1 noticeably suppressed invasive ability of both cell lines (Fig. 3G). These results indicate an oncogenic role of circPVT1 in NSCLC progression.

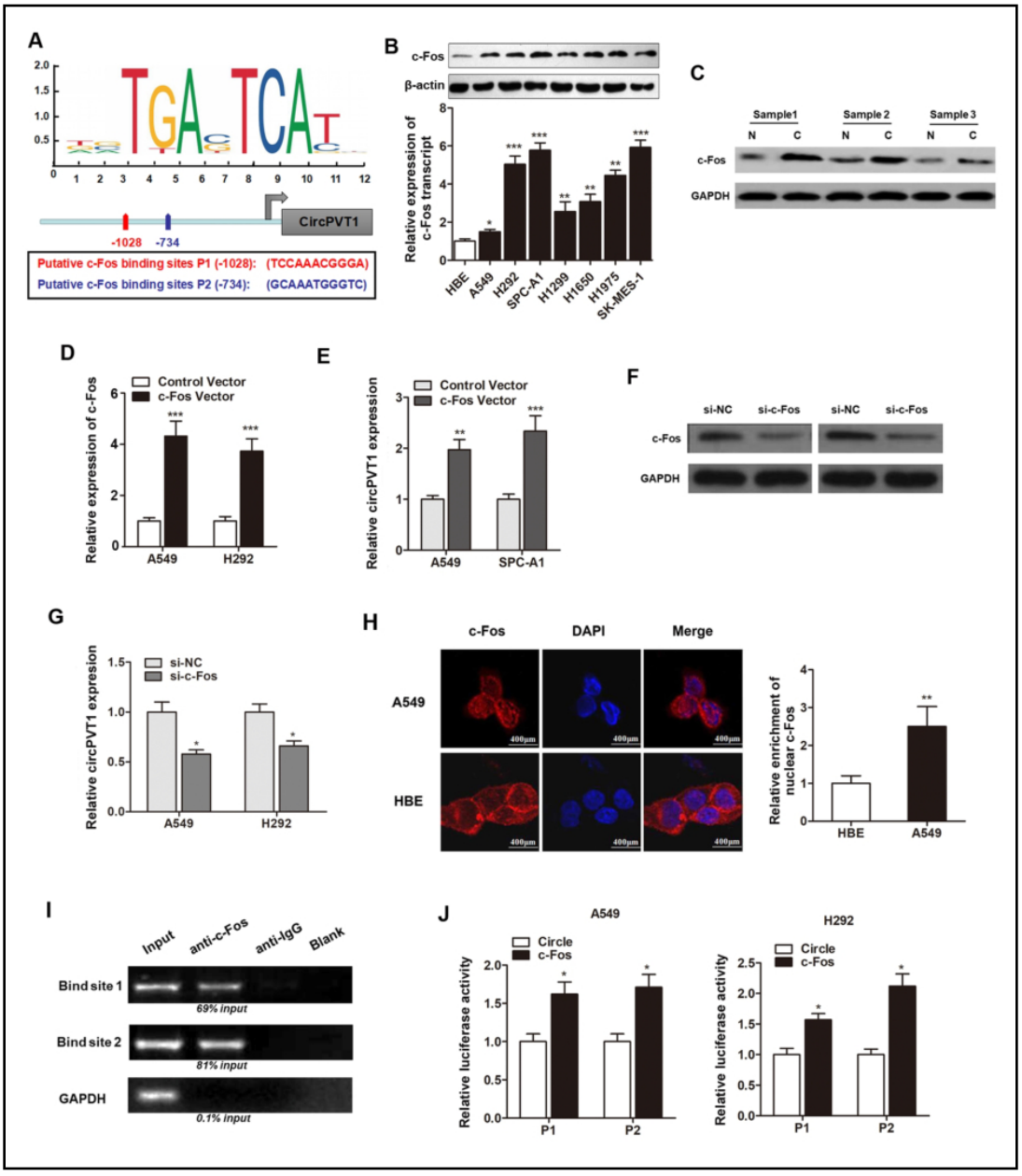

Fig. 2. CircPVT1 is actively induced by c-Fos in NSCLC cells. A Presentation of potential binding sequences at promoter region of circPVT1 by c-Fos by using the online transcription factor prediction software JASPAR. B. Determination of relative expression level of c-Fos in NSCLC cells at transcript (lower panel) and protein (upper panel) levels. C. Western blot experiment was used to detect the expression level of c-Fos protein in 3 NSCLC tissues and paired non-tumor tissues (C, cancer; N, non-tumor). D. Validation of c-Fos overexpression vector via RT-qPCR. E. CircPVT1 was measured in NSCLC cells via qPCR upon transfection of c-Fos vector. F. Western blot analysis of c-Fos protein level upon transfection of si-c-Fos. G. CircPVT1 was measured in NSCLC cells via qPCR upon transfection of si-c-Fos. H. Nuclear enrichment of c-Fos in A549 and HBE cells by immunofluorescence assay. I. Enrichment of c-Fos at circPVT1 promoter region in A549 cells by using specific primers after ChIP experiment. J. Dual-luciferase reporter analysis was used to verify the interaction between c-Fos and circPVT1 promoter. $^{*}P<0.05$, $^{**}P<0.01$, $^{***}P<0.001$.

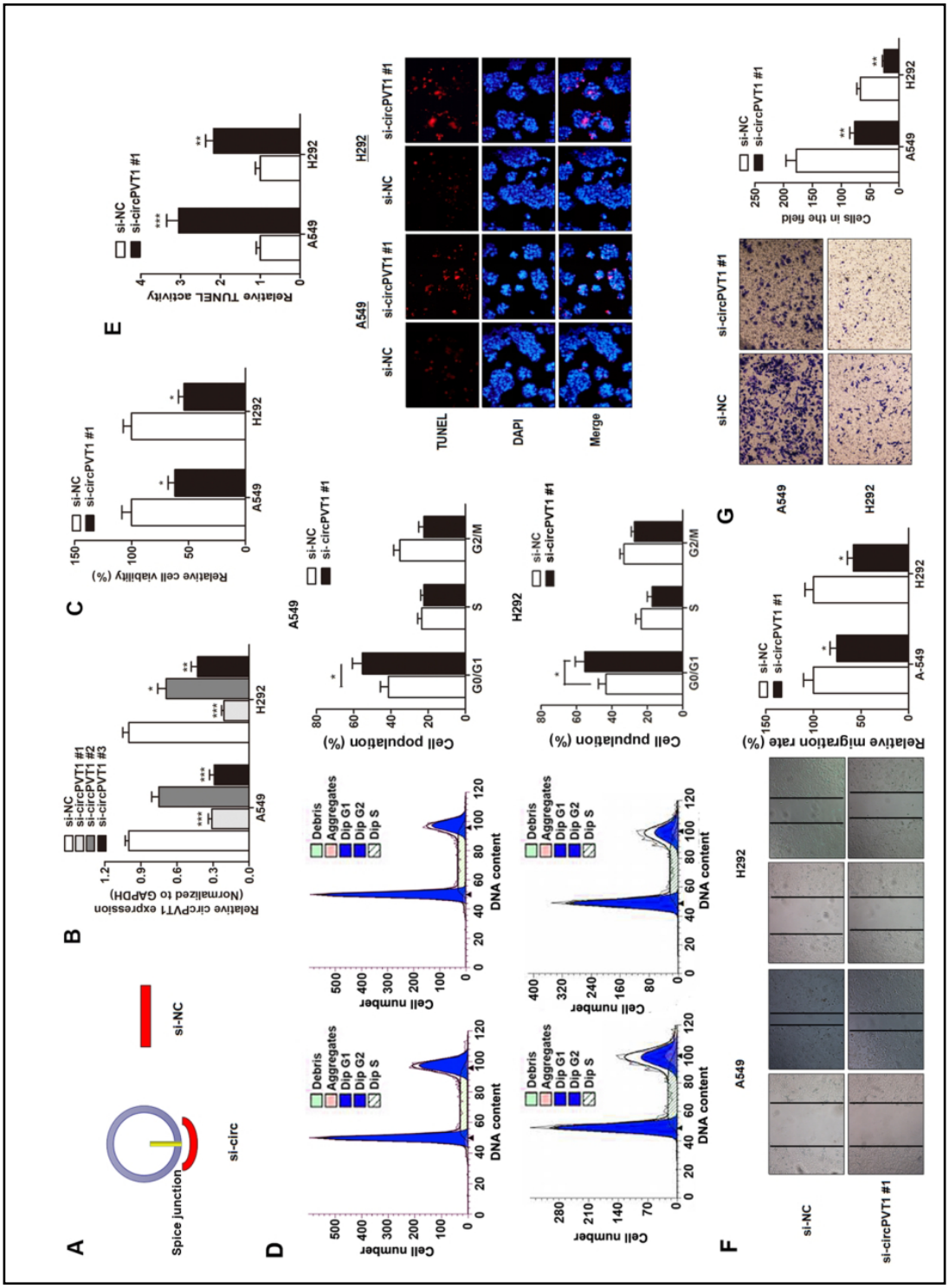

Fig. 3. Functional relevance between circPVT1 expression and NSCLC. A The sketch of structures of si-circPVT1 and si-NC vector are shown. B. The silencing effects were identified as by qPCR. C. Effect of circPVT1-knockdown on cell viability as detected by CCK8 assay. D. The influence induced by knockdown of circPVT1 on cell cycle mode are shown. E. Cell apoptosis in nucleus were tested by TUNEL assay upon knockdown of circPVT1. F-G. Cell migration and invasion ability was influenced by circPVT1-knockdown as shown in Wound-healing assay (F) and Matrigel-invasion assay (G), respectively. *P<0.05, **P<0.01, ***P<0.001.

E2F2 signaling pathway is responsible for circPVT1-mediated NSCLC progression

To determine how circPVT1 contributes to NSCLC progression, we used Signal Reporter Array to simultaneously investigate the activity changes of 45 canonical signaling pathways in A549 cells upon transfection of si-circPVT1 #1. Of note, we identified E2F reporter as one of the most significantly silenced pathways upon knockdown of circPVT1 (Fig. 4A). RT-qPCR experiments confirmed that E2F2 gene was upregulated in primary NSCLC tissues in contrast to non-tumor tissues, while no expression change was identified for E2F1 and E2F3 (Fig. 4B-4D). Western blot showed that knockdown of circPVT1 repressed E2F2 and E2F2-related protein expressions (Fig. 4E). To verify circPVT1 regulates NSCLC progression through targeting E2F2 signaling, we performed gain-and-loss functional assays by generating E2F2 overexpression vector (Fig. 4F). The suppressed cell viability caused by si-PVT1 #1 was dramatically reversed by co-transfection with E2F2 vector (Fig. 4G). Also, enhanced expression of E2F2 abrogated the effect of circPVT1 knockdown on cell invasion (Fig. 4H). Therefore, we demonstrated that circPVT1 promoted cell proliferation and invasion via targeting E2F2.

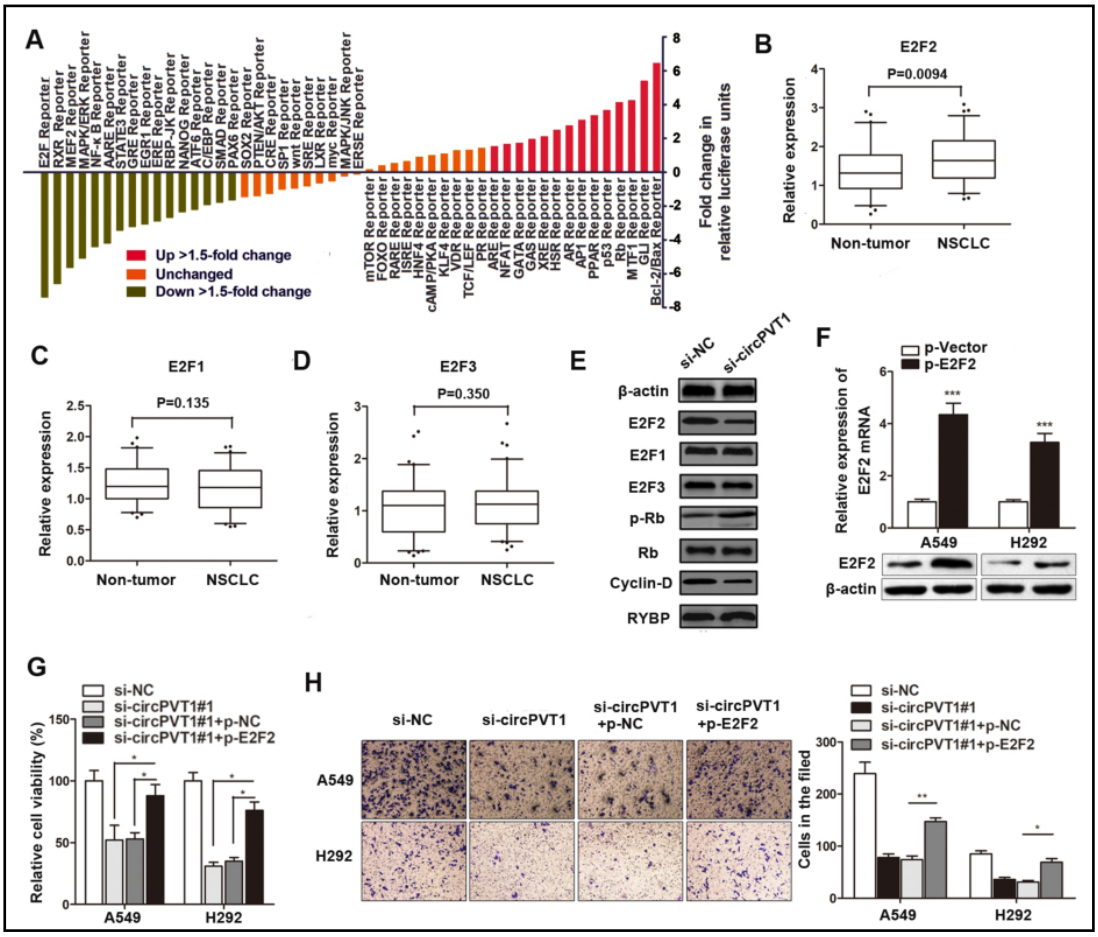

Fig. 4. CircPVT mediates NSCLC progression via regulating E2F2 pathway. A Histogram shows the fold changes for the activities of different signaling pathways in A549 cells after si-circPVT1, as indicated by reporter activity. B-D. RT-qPCR was used to detect the expression level of E2F1, E2F2 and E2F3 in NSCLC tissues and paired non-cancer tissues. E. The effect of circPVT1 on E2F2 signaling pathway in A549 cells was detected via Western blot. F. Verification of E2F2 overexpression plasmid in NSCLC cells. G. Cell viability was evaluated by CCK8 assay after co-transfection of si-circPVT1 and pcDNA-E2F2. H. Cell invasion was determined upon co-treatment of circPVT1 knockdown and E2F2 overexpression. $^{*}P<0.05$, $^{**}P<0.01$, $^{***}P<0.001$.

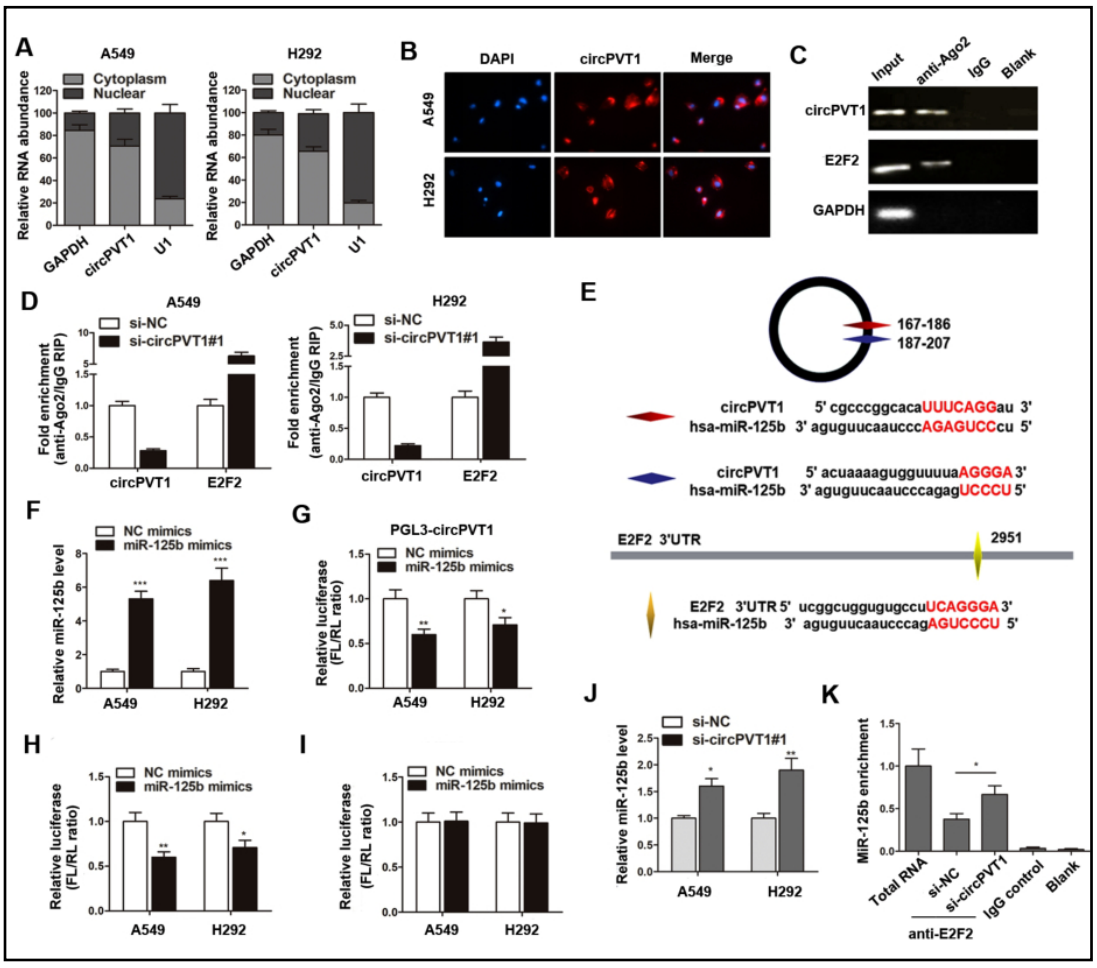

Fig. 5. CircPVT1 mediates E2F2 expression via serving as a ceRNA for miR-125b. A The expression level of circPVT1 in nuclear and cytoplasm of NSCLC cells. U1 (nuclear retained) and GAPDH (exported to cytoplasm) were used as controls. B. FISH analysis of the subcellular location of circPVT1 with specific probe in NSCLC cells. C. RIP experiments were performed using the AGO2 antibody, and specific primers were used to detect the enrichment of circPVT1 and E2F2 in A549 cells. D. RIP assay of the enrichment of Ago2 on circPVT1 and E2F2 transcripts relative to IgG in NSCLC cells transfected with si-circPVT1 #1. E. The putative sequences of miR-125b and circPVT1 with two binding sites (upper panel), miR-125b and E2F2 with one binding site (lower panel). F. Overexpression of miR-125b by miR-125b mimics was validated by qPCR. G-I. Firefly luciferase activity normalized to Renilla luciferase activity (FL/RL) in NSCLC cells co-transfected with luciferase reporters with wild type transcripts of circPVT1 (G), E2F2 (H), and mutant type transcript E2F2 (I). miR-125b was overexpressed by miR-125b mimics to test the influence on luciferase activity. J miR-125b expression was measured by qPCR in NSCLC cells upon knockdown of circPVT1. K. RIP was performed in cells downregulated circPVT1 using a E2F2 antibody to immunoprecipitate RNA and a primer to detect miR-125b. $^{*}P<0.05$, $^{**}P<0.01$, $^{***}P<0.001$.

CircPVT1 mediates E2F2 expression via serving as a ceRNA for miR-125b

It is widely accepted that circRNAs may function as competing endogenous RNAs (ceRNAs) to regulate the target mRNA of miRNAs. To test this hypothesis, we localized the subcellular location of circPVT1 in NSCLC cells. RT-qPCR analysis of nuclear and cytoplasmic circRNA showed that circPVT1 was enriched in cytoplasm section of A549 and H292 cells (Fig. 5A). Fluorescent in situ hybridization of circPVT1 with specific probe further confirmed that circPVT1 was mainly distributed in the cytoplasm section (Fig. 5B). To confirm circPVT1 exerts this effect through associating with E2F2 targeting miRNAs, we performed RIP assay on Ago2, which is the core component of the RNA-induced mediating complex. Clearly, both

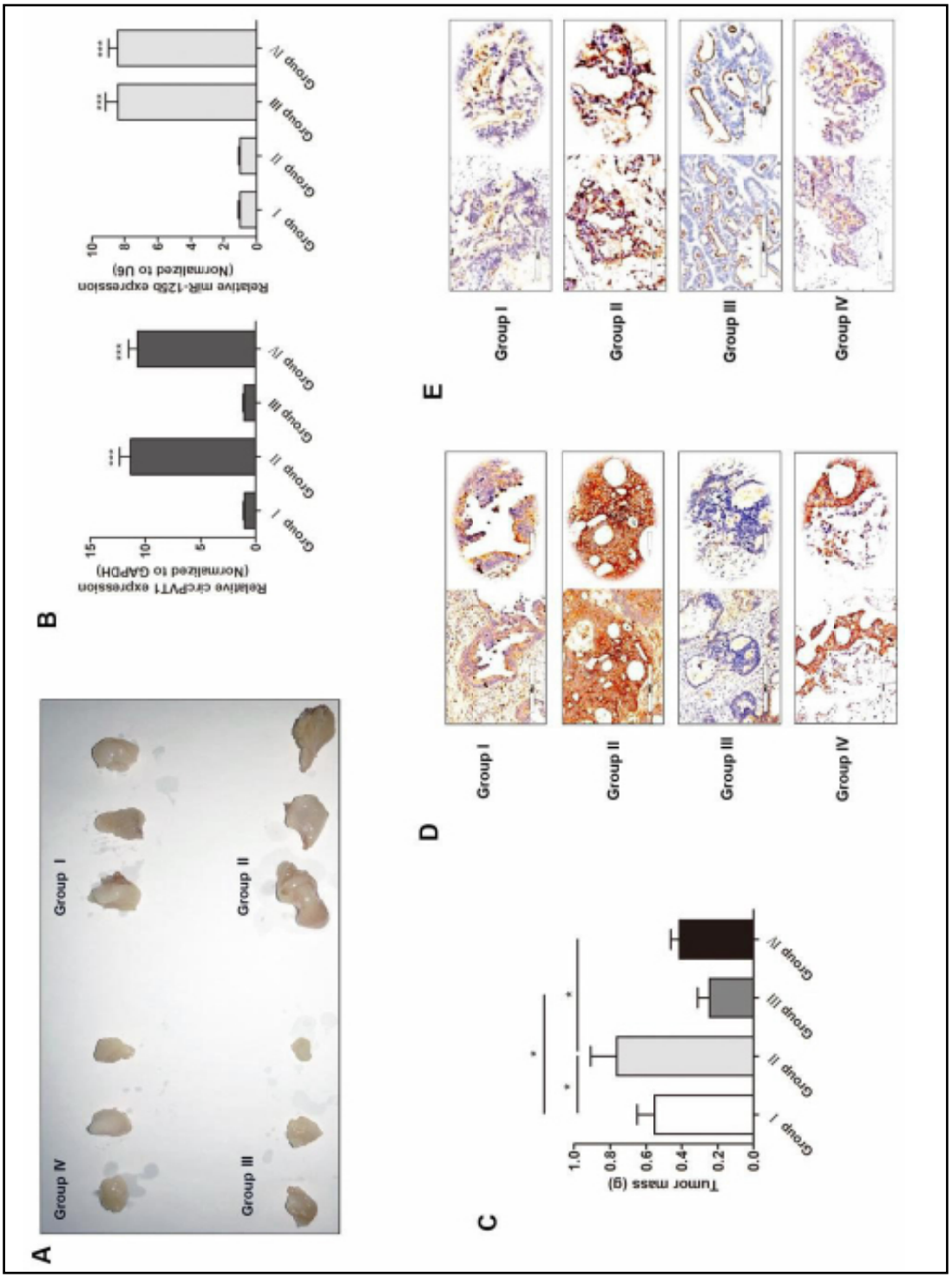

Fig. 6. CircPVT1 mediates NSCLC tumorigenesis via miR-125b in vivo. A Photographs of tumors that developed in xenograft transplanted nude mouse tumor models. Group I (Lv-NC + Lv-SC), Group II (Lv-circPVT1 + Lv-SC), Group III (Lv-NC + Lv-miR-125b) and Group IV (Lv-circPVT1 + Lv-miR-125b). B. The expression levels of circPVT1 and miR-125b were measured by qPCR in xenograft groups. C. Weights of tumors that developed in xenografts from respective groups. D. IHC analysis of expression levels of E2F2 in respective groups. E. IHC analysis of expression levels of Ki-67 in respective groups. *P<0.05, ***P<0.001.

circPVT1 and E2F2 were enriched with Ago2 (Fig. 5C). In addition, knockdown of circPVT1 resulted in a decreased enrichment between Ago2 and cricPVT1 but elicited an increase recruitment of Ago2 to E2F2 transcript (Fig. 5D), indicating that circPVT1 could compete with E2F2 transcripts for the Ago2-based miRNA-mediated silencing complex.

Subsequently, we verified the miRNAs that participated in the sponge of circPVT1 and E2F2 pathway. Interestingly, a microRNA, namely miR-125b, was predicted to target both E2F2 and circPVT1 by miRanda (*http://www.microrna.org/microrna/home.do*) and TargetScan (*http://www.targetscan.org/*) (Fig. 5E). By generating miR-125b mimics and cloning wild or mutant 3'-UTR of E2F2/circPVT1 downstream into PGL3 luciferase reporters, we performed luciferase reporter assay to detect the sponge of miR-125b with both reporters (Fig. 5F). As expected, luciferase activity was significantly suppressed by overexpression of miR-125b at both circPVT1 and E2F2 wild type reporter, but little effect was observed with mutant E2F2 reporters (Fig. 5G-I). In addition, miR-125b was upregulated in NSCLC cells when circPVT1 was silenced by si-circPVT1#1 (Fig. 5J). RIP experiment revealed that silence of circPVT1 promoted the enrichment of miR-125b bound to E2F2 (Fig. 5K). Taken together, our results showed that circPVT1 serves as a molecular sponge for miR-125b to modulate the expression of E2F2.

CircPVT1 mediates tumorigenesis through sponging miR-125b and upregulating E2F2 in vivo

Following the above observations, we further verified these *in vitro* findings by using an *in vivo* xenograft model. A549 cells that stably transfected with lentiviras vector containing circPVT1 plasmid (Lv-circPVT1), miR-125b (Lv-miR-125b) and respective negative control vectors were injected into the flanks of nude mice. Herein, mice xenograft carrying four groups of transfected cells were established: Group I (Lv-NC + Lv-SC), GroupII (Lv-circPVT1 + Lv-SC), Group III (Lv-NC + Lv-miR-125b), Group IV (Lv-circPVT1 + Lv-miR-125b). More than three mice in each group were remained after excluding mice that were dead or with complications, such as skin necrosis due to infection. Tumors were stripped and tumor mass were quantified (Fig. 6A). The expression levels of circPVT1 and miR-125b in each group were verified (Fig. 6B). The quantitative data showed that overexpression of circPVT1 promoted tumor growth (Group II vs. Group I), while overexpression of miR-125b repressed the growth effect (Group III vs. Group I). Moreover, co-infection of Lv-miR-125b reversed the enhancement induced by Lv-circPVT1 (Group IV vs. Group II, Fig. 6C). In addition, immunohistochemistry (IHC) analysis was conducted to determine the expression level of E2F2 in xenograft tissues. As shown in Fig. 6D, circPVT1 upregulated-, while miR-125b inhibited the expression level of E2F2. IHC analysis also showed that circPVT1/miR-125b pathway affected the cell proliferation marker Ki-67 in xenograft tissues (Fig. 6E).

Discussion

Extensive efforts in the past have contributed to the understanding of both molecular and cellular mechanisms of noncoding RNAs in cancer progression, however, nearly all patients with lung cancer invariably become metastatic and chemoresistant [20]. Thus, novel molecular signatures seem to hold great promise in tumor characterization and could be used as potential prognostic markers and treatment target [21]. To identify potential molecular markers for NSCLC, we focused on circular RNAs, a group of recently identified transcripts formed by exon skipping or back-splicing events, and investigated the functional correlation between NSCLC progression and circPVT1 in NSCLC. Our own date showed that circPVT1 was upregulated in NSCLC partially due to the activation of c-Fos. Moreover, circPVT1 promotes NSCLC progression via the sponge of miR-125b and activating the downstream E2F2 pathway (Fig. 7).

Several attempts have been made to use miRNAs or lncRNAs in serum or plasma as useful predictors [22, 23]. Nevertheless, these potential tumor biomarkers are often in relatively low abundance and degradation easily occurs. The existence of circular form of RNAs in body fluid was firstly reported by Sanger et al. in 1976. they demonstrated that this type of single-stranded closed circular RNA was stably expressed from viroids to certain highest species, such as human beings [24]. With the development of gene investigations, it is recognized that circRNAs are widely expressed in human cells, and their expression levels can be 10-fold or higher compared to their linear isomers. The two most important properties of circRNAs are highly conserved sequences and a high degree of stability in mammalian cells [25]. More importantly, circRNAs are a class of endogenous RNAs featuring stable structure making them avoid exonucleolytic degradation by RNase R. Compared with other noncoding RNA, such as miRNAs and lncRNAs, these properties provide circRNAs with the potential to become ideal biomarkers in the diagnosis and prognosis of cancers [26, 27]. In this study, we showed that circPVT1 was significantly upregulated in NSCLC and correlated with clinical diagnosis. Therefore, circPVT1 may serve as a novel biomarker used for early diagnosis, treatment monitoring and prognosis for NSCLC patients.

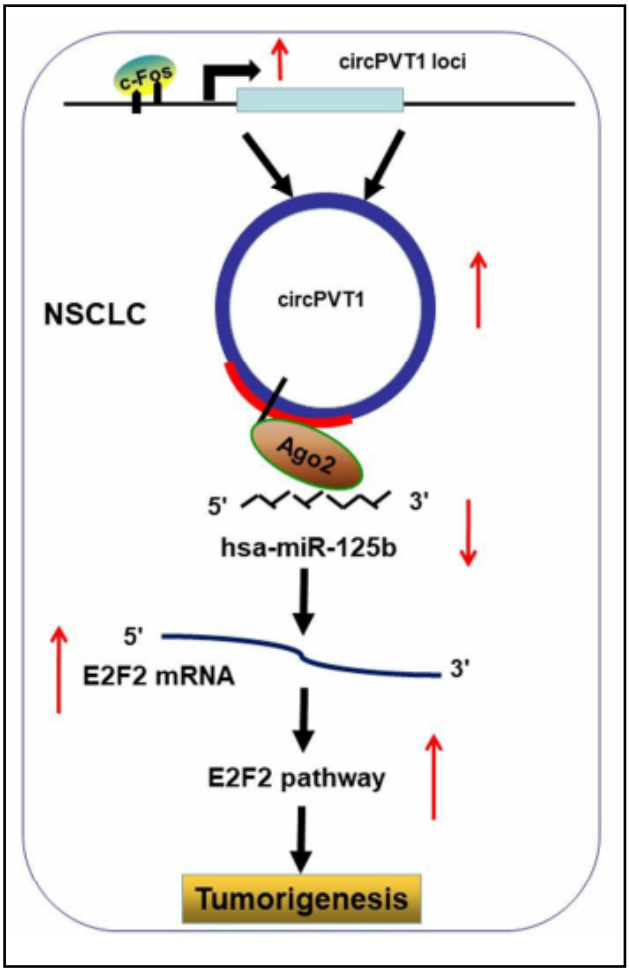

Fig. 7. Schematic representation of the proposed mechanism of circPVT1 in NSCLC cells. CircPVT1 acted as a miR-125b sponge to regulate the miR-125b/E2F2 pathway. c-Fos-induced upregulation of circPVT1 in NSCLC decreased the activity of miR-125b, which increased the expression of E2F2 and the downstream effectors, thereby promoting NSCLC tumorigenesis and progression.

The functional role of circPVT1 in cancer progression and other diseases were reported in several previous studies. Chen et al. demonstrated that circPVT1 promotes cell proliferation and serves as a prognostic factor in gastric cancer [17]. Verduci et al. also revealed an oncogenic role of circPVT1 in head and neck squamous cell carcinoma through the mutant p53/YAP/TEAD transcription-competent complex [16]. In addition, Panda et al. found that circPVT1 is a senescence-associated circular RNA, and it is elevated in dividing cells and reduced in senescent cells, sequesters let-7 to enable a proliferative phenotype [18]. The specific role of circPVT1 in lung cancer is still unknown. In this study, we revealed that circPVT1 plays an oncogenic role in NSCLC by regulating cell growth and metastasis, which is consistent with previous reports. In addition, transcription factor c-Fos was identified as a specific transcription activator for circPVT1, and induced the upregulation of circPVT1.

To get a deeper understanding of the role of circPVT1 in NSCLC, we performed Signal Reporter Array to determine the downstream pathway that account for the functional effects induced by circPVT1, and E2F2 was identified as a direct target of circPVT1. E2F2 is a member of the E2F family of transcription factors and binds DNA cooperatively with DPDP1-polypeptide through the E2 recognition site in the promoter region of genes to produce products involved in cell cycle regulation, DNA replication and metastasis [28, 29]. The oncogenic property of E2F2 is observed in multiple cancers due to its effect on promoting cell-cycle progression. Overexpressed E2F2 is a crucial center of cell cycle regulation in NSCLC cancer and high expression of E2F2 is significantly associated with poor prognosis [30]. The studies of E2F2 with EMT, previously associated with metastases and chemoresistance are contradictory [31-33]. Our current study suggested that E2F2 was upregulated in NSCLC, and E2F2 was responsible for the circPVT1 mediated NSCLC carcinogenesis. Take a step further, we localized the sub-cellular distribution of circPVT1 in NSCLC cells. We found that circPVT1 was enriched in cytoplasm section. It is well known that circRNAs located in cytoplasm may function as miRNA sponges, thus indirectly mediate the expression level of targeted mRNA [34]. Our comprehensive analysis of bioinformatics combined luciferase reporter assay and immunoprecipitation experiments verified miR-125b as a sponge target of both circPVT1 and E2F2 gene, and was responsible for the circPVT1-mediated NSCLC progression *in vivo*. Therefore, our date comprehensively demonstrated an oncogenic role of circPVT1 through sponging miR-125b and releasing E2F2.

We should admit that our research can be more meaningful provided that we complete the date supporting a survival and prognostic conclusion in NSCLC patients. We have been collecting survival results and will develop relevant conclusions in our future works.

Conclusion

In summary, our findings revealed that c-Fos-activated circPVT1 plays an oncogenic role in NSCLC by acting as a ceRNA. Therefore, circPVT1 may be considered as a diagnostic biomarker and therapeutic target for NSCLC patients, enhancing the clinical benefits.

Acknowledgements

This study was funded by Science and technology research project of Heilongjiang Provincial Department of Education (12541848) and Research project of Heilongjiang Provincial Health and Family Planning Commission (2016-398).

Disclosure Statement

The authors declare that they have no competing interests.

References

1 Torre LA, Bray F, Siegel RL, Ferlay J, Lortet-Tieulent J, Jemal A: Global cancer statistics, 2012. CA Cancer J Clin 2015;65:87-108.
2 Herth FJ, Eberhardt R: Flexible bronchoscopy and its role in the staging of non-small cell lung cancer. Clin Chest Med 2010;31:87-100.
3 Pastorino U: Lung cancer screening. Br J Cancer 2010;102:1681-1686.
4 Gettinger S, Lynch T: A decade of advances in treatment for advanced non-small cell lung cancer. Clin Chest Med 2011;32:839-851.

5 Liang D, Wilusz JE: Short intronic repeat sequences facilitate circular RNA production. Genes Dev 2014;28:2233-2247.
6 Chen LL, Yang L: Regulation of circRNA biogenesis. RNA Biol 2015;12:381-388.
7 Lasda E, Parker R: Circular RNAs: diversity of form and function. RNA 2014;20:1829-1842.
8 Ivanov A, Memczak S, Wyler E, Torti F, Porath HT, Orejuela MR, Piechotta M, Levanon EY, Landthaler M, Dieterich C, Rajewsky N: Analysis of intron sequences reveals hallmarks of circular RNA biogenesis in animals. Cell Rep 2015;10:170-177.
9 Zhou B, Yu JW: A novel identified circular RNA, circRNA_010567, promotes myocardial fibrosis via suppressing miR-141 by targeting TGF-beta1. Biochem Biophys Res Commun 2017;487:769-775.
10 Zhang HD, Jiang LH, Sun DW, Hou JC, Ji ZL: CircRNA: a novel type of biomarker for cancer. Breast Cancer 2018;25:1-7.
11 Yao JT, Zhao SH, Liu QP, Lv MQ, Zhou DX, Liao ZJ, Nan KJ: Over-expression of CircRNA_100876 in non-small cell lung cancer and its prognostic value. Pathol Res Pract 2017;213:453-456.
12 Tseng YY, Moriarity BS, Gong W, Akiyama R, Tiwari A, Kawakami H, Ronning P, Reuland B, Guenther K, Beadnell TC, Essig J, Otto GM, O'Sullivan MG, Largaespada DA, Schwertfeger KL, Marahrens Y, Kawakami Y, Bagchi A: PVT1 dependence in cancer with MYC copy-number increase. Nature 2014;512:82-86.
13 Wang F, Yuan JH, Wang SB, Yang F, Yuan SX, Ye C, Yang N, Zhou WP, Li WL, Li W, Sun SH: Oncofetal long noncoding RNA PVT1 promotes proliferation and stem cell-like property of hepatocellular carcinoma cells by stabilizing NOP2. Hepatology 2014;60:1278-1290.
14 Wan L, Sun M, Liu GJ, Wei CC, Zhang EB, Kong R, Xu TP, Huang MD, Wang ZX: Long Noncoding RNA PVT1 Promotes Non-Small Cell Lung Cancer Cell Proliferation through Epigenetically Regulating LATS2 Expression. Mol Cancer Ther 2016;15:1082-1094.
15 Memczak S, Jens M, Elefsinioti A, Torti F, Krueger J, Rybak A, Maier L, Mackowiak SD, Gregersen LH, Munschauer M, Loewer A, Ziebold U, Landthaler M, Kocks C, le Noble F, Rajewsky N: Circular RNAs are a large class of animal RNAs with regulatory potency. Nature 2013;495:333-338.
16 Verduci L, Ferraiuolo M, Sacconi A, Ganci F, Vitale J, Colombo T, Paci P, Strano S, Macino G, Rajewsky N, Blandino G: The oncogenic role of circPVT1 in head and neck squamous cell carcinoma is mediated through the mutant p53/YAP/TEAD transcription-competent complex. Genome Biol 2017;18:237.
17 Chen J, Li Y, Zheng Q, Bao C, He J, Chen B, Lyu D, Zheng B, Xu Y, Long Z, Zhou Y, Zhu H, Wang Y, He X, Shi Y, Huang S: Circular RNA profile identifies circPVT1 as a proliferative factor and prognostic marker in gastric cancer. Cancer Lett 2017;388:208-219.
18 Panda AC, Grammatikakis I, Kim KM, De S, Martindale JL, Munk R, Yang X, Abdelmohsen K, Gorospe M: Identification of senescence-associated circular RNAs (SAC-RNAs) reveals senescence suppressor CircPVT1. Nucleic Acids Res 2017;45:4021-4035.
19 Zhang S, Zhu D, Li H, Li H, Feng C, Zhang W: Characterization of circRNA-Associated-ceRNA Networks in a Senescence-Accelerated Mouse Prone 8 Brain. Mol Ther 2017;25:2053-2061.
20 Li P, Zhang X, Wang H, Wang L, Liu T, Du L, Yang Y, Wang C: MALAT1 Is Associated with Poor Response to Oxaliplatin-Based Chemotherapy in Colorectal Cancer Patients and Promotes Chemoresistance through EZH2. Mol Cancer Ther 2017;16:739-751.
21 Li P, Zhang X, Wang L, Du L, Yang Y, Liu T, Li C, Wang C: lncRNA HOTAIR Contributes to 5FU Resistance through Suppressing miR-218 and Activating NF-kappaB/TS Signaling in Colorectal Cancer. Mol Ther Nucleic Acids 2017;8:356-369.
22 Wang ZX, Bian HB, Wang JR, Cheng ZX, Wang KM, De W: Prognostic significance of serum miRNA-21 expression in human non-small cell lung cancer. J Surg Oncol 2011;104:847-851.
23 Xu N, Chen F, Wang F, Lu X, Wang X, Lv M, Lu C: Clinical significance of high expression of circulating serum lncRNA RP11-445H22.4 in breast cancer patients: a Chinese population-based study. Tumour Biol 2015;36:7659-7665.
24 Sanger HL, Klotz G, Riesner D, Gross HJ, Kleinschmidt AK: Viroids are single-stranded covalently closed circular RNA molecules existing as highly base-paired rod-like structures. Proc Natl Acad Sci U S A 1976;73:3852-3856.
25 Guo JU, Agarwal V, Guo H, Bartel DP: Expanded identification and characterization of mammalian circular RNAs. Genome Biol 2014;15:409.
26 Huang YS, Jie N, Zou KJ, Weng Y: Expression profile of circular RNAs in human gastric cancer tissues. Mol Med Rep 2017;16:2469-2476.

27 Wang H, Xiao Y, Wu L, Ma D: Comprehensive circular RNA profiling reveals the regulatory role of the circRNA-000911/miR-449a pathway in breast carcinogenesis. Int J Oncol 2018;52:743-754.
28 Ahn JD, Morishita R, Kaneda Y, Kim HS, Chang YC, Lee KU, Park JY, Lee HW, Kim YH, Lee IK: Novel E2F decoy oligodeoxynucleotides inhibit *in vitro* vascular smooth muscle cell proliferation and *in vivo* neointimal hyperplasia. Gene Ther 2002;9:1682-1692.
29 Chang X, Yue L, Liu W, Wang Y, Wang L, Xu B, Wang Y, Pan J, Yan X: CD38 and E2F transcription factor 2 have uniquely increased expression in rheumatoid arthritis synovial tissues. Clin Exp Immunol 2014;176:222-231.
30 Feliciano A, Garcia-Mayea Y, Jubierre L, Mir C, Hummel M, Castellvi J, Hernandez-Losa J, Paciucci R, Sansano I, Sun Y, Ramon YCS, Kondon H, Soriano A, Segura M, Lyakhovich A, ME LL: miR-99a reveals two novel oncogenic proteins E2F2 and EMR2 and represses stemness in lung cancer. Cell Death Dis 2017;8:e3141.
31 Gu K, Li MM, Shen J, Liu F, Cao JY, Jin S, Yu Y: Interleukin-17-induced EMT promotes lung cancer cell migration and invasion via NF-kappaB/ZEB1 signal pathway. Am J Cancer Res 2015;5:1169-1179.
32 Liu X, Tseng SC, Zhang MC, Chen SY, Tighe S, Lu WJ, Zhu YT: LIF-JAK1-STAT3 signaling delays contact inhibition of human corneal endothelial cells. Cell Cycle 2015;14:1197-1206.
33 Yuwanita I, Barnes D, Monterey MD, O'Reilly S, Andrechek ER: Increased metastasis with loss of E2F2 in Myc-driven tumors. Oncotarget 2015;6:38210-38224.
34 Zhu Z, Li Y, Liu W, He J, Zhang L, Li H, Li P, Lv L: Comprehensive circRNA expression profile and construction of circRNA-associated ceRNA network in fur skin. Exp Dermatol 2018;27:251-257.